Absence of the Twisted Superfluid Phase in a mean field model of bosons on a Honeycomb Lattice

Sayan Choudhury[1,*] and Erich J Mueller[1,†]

[1] *Laboratory of Atomic and Solid State Physics, Cornell University, Ithaca, New York*

(Dated: November 21, 2012)

Motivated by recent observations (P. Soltan-Panahi *et al.*, Nature Physics **8**, 71-75 (2012)), we study the stability of a Bose-Einstein Condensate within a spin-dependent honeycomb lattice towards forming a "Twisted Superfluid phase". Our exhaustive numerical search fails to find this phase, pointing to possible non-mean field physics.

PACS numbers: 03.75.Hh, 03.75.Mn, 67.85.Hj, 03.75.-b, 67.85.-d

I. INTRODUCTION

A. Background

Recently Soltan-Panahi *et al.* found evidence of a zero quasi-momentum "Twisted Superfluid (TSF) phase" of a two-component Bose-Einstein condensate (BEC) trapped in a spin-dependent honeycomb lattice [1]. A TSF is characterized by Bose-Einstein condensation into a state whose order parameter (a macroscopically occupied single particle wavefunction) has a spatially varying phase. The simplest example is condensation at finite momentum. Alternatively, in a non-Bravais lattice where the unit cell involves multiple sites, one can have a TSF at zero quasi-momentum if the phase of the order parameter varies throughout the unit cell. We model Soltan-Panahi et al.'s experiment [1] with a mean field Gross-Pitaevskii function. We find that the TSF phase is absent within mean field theory thus suggesting that the observations are due to non-mean field effects.

Twisted Superfluid phases are quite exotic; the phase twists are naturally associated with microscopic currents. Moreover, the present example involves spontaneous symmetry breaking, and provides a setting for studying phase transition physics. Analogous physics can be found in magnetic systems [2] and in the excited states of lattice bosons [3, 4].

To see the connection between TSF and currents, consider a hopping model on a honeycomb lattice :

$$H = -\mathrm{t}\sum_{\langle \mathrm{ij}\rangle} \hat{\mathrm{a}}_\mathrm{i}^\dagger \hat{\mathrm{a}}_\mathrm{j} + \hat{\mathrm{a}}_\mathrm{j}^\dagger \hat{\mathrm{a}}_\mathrm{i}, \tag{1}$$

where $\hat{\mathrm{a}}_\mathrm{i}$ annihilates a boson on site i, t is the energy scale of hopping and $\langle \mathrm{ij}\rangle$ represent nearest neighbor sites.The rate of change of the density on site i is :

$$\Gamma_\mathrm{i} = \frac{\mathrm{d}}{\mathrm{dt}}\langle \hat{\mathrm{n}}_\mathrm{i}\rangle = \sum_{<\text{neighbours j}>} -\mathrm{t}\ \mathrm{Im} < \hat{\mathrm{a}}_\mathrm{i}^\dagger \hat{\mathrm{a}}_\mathrm{j} >, \tag{2}$$

and one interprets $-\mathrm{t}\ \mathrm{Im} < \hat{\mathrm{a}}_\mathrm{i}^\dagger \hat{\mathrm{a}}_\mathrm{j} >$ as the net current flowing from site j to site i. In the case of a condensed system, the operators $\hat{\mathrm{a}}_\mathrm{i}$ can be replaced by c-numbers and any non-trivial phases give rise to currents.

The experimental evidence suggests that the order parameter is uniform on each of the triangular sub-lattices of the honeycomb lattice :

$$\langle \hat{\mathrm{a}}_{\mathrm{j}\pm}\rangle = \sqrt{\mathrm{n}_\pm}\exp(\pm \mathrm{i}\ \delta/2), \tag{3}$$

where the + and - signs are taken on the two distinct sub-lattices. For the simple model in eq.(1), $\frac{\mathrm{d}}{\mathrm{dt}}\mathrm{n_i} = \pm 3\ \mathrm{t}\ \sqrt{\mathrm{n_+ n_-}}\ \mathrm{Sin}(\delta)$, and the density is not stationary unless $\delta = 0$ or π. This argument misses the role of interactions and is therefore incomplete. In particular, interactions can give a $\mathrm{Sin}(2\delta)$ contribution to Γ_i, and yield steady state for $\delta \neq 0$ or π. This can be interpreted as counter-flowing single particle and pair currents which yield zero net flow (see Section V). Regardless of the interpretation, the sub-lattice phase, δ is worthy of study.

B. Experimental Evidence

Soltan-Panahi *et al.*'s evidence for non-trivial phases comes from time-of-flight (TOF) expansion, a technique where all trapping fields are removed and the atomic ensemble falls freely under gravity. Neglecting interactions [7], the long-time real space density profile is simply the initial density in momentum space. For the special case of a BEC, $n_k = |\psi(\mathbf{k})|^2 = |\int \exp(+i\mathbf{k}.\mathbf{r})\psi(\mathbf{r})|^2$ and the time-of-flight density profile is the squared modulus of the Fourier transform of the order parameter, $\psi(\mathbf{r})$. As schematically illustrated in Figure 1, if $\psi(\mathbf{r})$ is real, and has the symmetry of the honeycomb lattice, its Fourier transform (and consequently the TOF pattern) is six fold symmetric. This symmetry persists even if the densities on the two sub-lattices differ, forming a three-fold symmetric charge density wave (CDW) as illustrated in Figure 2. This six-fold rotational symmetry of the TOF pattern is a consequence the point group symmetry of the lattice (C_{3v}) and the relation $\psi(-\mathbf{k}) = \psi^*(\mathbf{k})$, which holds for

* sc2385@cornell.edu
† em256@cornell.edu

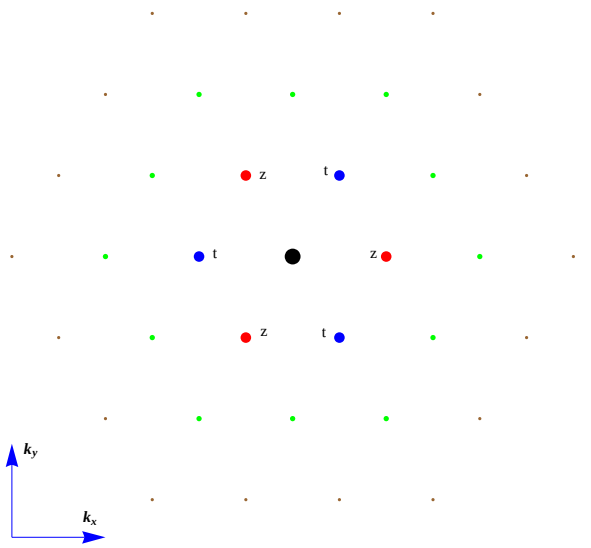

FIG. 1. Schematic of the Time-of-Flight (TOF) pattern for a superfluid in a 2D honeycomb lattice. Larger darker dots correspond to more particles with a given momentum. The complex numbers t and z represent the amplitudes of the Fourier transform of the condensate wavefunction at $k = (\frac{\pi}{a}, 0)$ and $k = (\frac{\sqrt{3}\pi}{2a}, \frac{\pi}{2a})$The twisted superfluid (TSF) is described by $|t| \neq |z|$.

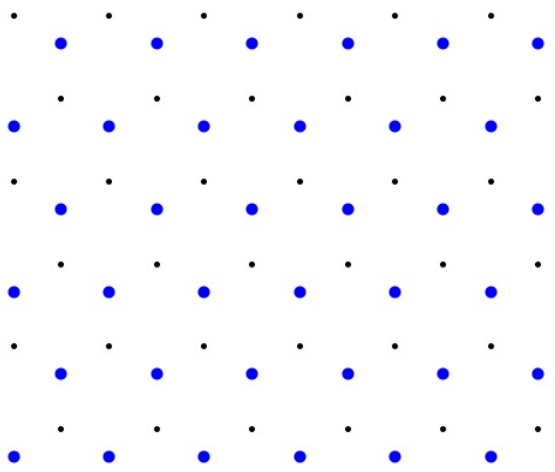

FIG. 2. The density wave formed in a honeycomb lattice for the $m_F = 1$ atoms. The points represent lattice sites. Larger points indicate more atoms. This pattern is periodically repeated. A complementary density wave is formed by $m_F = -1$ atoms. This density wave does not lead to a 6-fold symmetry breaking in TOF unless additional phases appear on the sites.

real $\psi(\mathbf{r})$. Therefore, if the TOF pattern becomes three-fold symmetric ($|t| \neq |z|$ in Figure 1), the real space wavefunction has different phases on the two sublattices. The experimentalists see exactly this signature.

Soltan-Panahi et al. work with a two-component mixture of ^{87}Rb atoms in a spin-dependent honeycomb lattice [1]. The two spin states can form out-of-phase CDWs. As was emphasized in [1] this density wave does not lead to the breakdown of the rotational symmetry in time-of-flight. The symmetry breaking was opposite for the two species (i.e $\frac{|t_1|}{|z_1|} = \frac{|z_2|}{|t_2|}$, where t, z denote the amplitudes of the TOF peaks in Fig. 1).

II. THE MODEL

Within a mean field model, we will investigate the relative stability of twisted or ordinary superfluids. The energy of a two component BEC, described by macroscopic wavefunctions ψ_1 and ψ_2 is :

$$E_{3D} = \int d^3\mathbf{r} \sum_{\sigma=1,2} \left[\frac{\hbar^2}{2m} |\nabla\psi_\sigma(\mathbf{r})|^2 + V_\sigma(\mathbf{r})|\psi_\sigma(\mathbf{r})|^2 \right] + \sum_{\sigma=1,2} \frac{U^\sigma_{3D}}{2} |\psi_1(\mathbf{r})|^4 + W_{3D}|\psi_1(\mathbf{r})|^2|\psi_2(\mathbf{r})|^2 + V_{\rm conf}(\mathbf{r})(|\psi_1(\mathbf{r})|^2 + |\psi_2(\mathbf{r})|^2) \quad (4)$$

Here, $U^\sigma_{3D} = \frac{4\pi\hbar^2 a_\sigma}{m}$ is the intra-species interaction energy (a_σ is the intra-species scattering length for species σ), while $W_{3D} = \frac{4\pi\hbar^2 a_{12}}{m}$ is the inter-species interaction energy (a_{12} is the inter-species scattering length). We focus on the case in [1], where the states 1 (described by ψ_1) and 2 (described by ψ_2) are the $|\mathrm{F} = 1, \mathrm{m_F} = 1\rangle$ and $|\mathrm{F} = 1, \mathrm{m_F} = -1\rangle$ states of ^{87}Rb. For these two hyperfine states of ^{87}Rb atoms, U^1_{3D},$U^2_{3D}$and W are almost equal ($\approx 100a_0$ where a_0 is the Bohr radius). In principle collisions can connect these hyperfine states to others (for example $|\mathrm{F} = 1, \mathrm{m_F} = 0\rangle$). For the experimental parameters, these processes are off-resonant and the two-component Bose gas model describes the physics.

In the experiment [1], the honeycomb lattice is generated by 3 lasers yielding a potential $V_i(\mathbf{r}) = V_{\rm hex}(\mathbf{r}) \pm \alpha B_{\rm eff}(\mathbf{r})$ where, state 1 sees the sign '+' and state 2 sees the sign '-' (with $\alpha = 0.13$) and

$$V_{\rm hex}(\mathbf{r}) = 2\ V_{\rm lat}(\mathrm{Cos}[\mathrm{k_L}\ \mathbf{b_1}.\mathbf{x}] + \mathrm{Cos}[\mathrm{k_L}\ \mathbf{b_2}.\mathbf{x}] + \mathrm{Cos}[\mathrm{k_L}\ \mathbf{b_3}.\mathbf{x}]) \quad (5)$$

$$B_{\rm eff}(\mathbf{r}) = 2\sqrt{3}\ V_{\rm lat}(\mathrm{Sin}[\mathrm{k_L}\ \mathbf{b_1}.\mathbf{x}] + \mathrm{Sin}[\mathrm{k_L}\ \mathbf{b_2}.\mathbf{x}] + \mathrm{Sin}[\mathrm{k_L}\ \mathbf{b_3}.\mathbf{x}]) \quad (6)$$

$$(7)$$

where, $\mathbf{b1} = -\frac{\mathbf{1}}{\mathbf{2}}\mathbf{e_x} - \frac{\sqrt{\mathbf{3}}}{\mathbf{2}}\mathbf{e_y}; \mathbf{b2} = \mathbf{e_x}; \mathbf{b3} = -\frac{\mathbf{1}}{\mathbf{2}}\mathbf{e_x} + \frac{\sqrt{\mathbf{3}}}{\mathbf{2}}\mathbf{e_y}$ and $\mathrm{k_L} = 2\sqrt{3}\pi/\lambda_{\rm L}$ (λ_L is the laser wavelength and is 830 nm for the experiment under discussion). With these considerations $V_{\rm lat}$ is the height of the barrier between neighboring sites. The difference between the maximum and minimum values of $V_{\rm hex}(\mathbf{r})$ is 4 $V_{\rm lat}$.

The experiment uses a separate set of lasers to provide strong confinement in the third dimension, $V_{\rm conf}(\mathbf{r})$:

$$V_{\rm conf}(\mathbf{r}) = \mathrm{V_{1D}}\ \mathrm{Cos}[\frac{2\pi}{\lambda_{\rm 1D}}\mathbf{z}] \approx \frac{\mathrm{V_{1D}}}{2}(\frac{2\pi}{\lambda_{\rm 1D}})^2\ \mathrm{z}^2. \quad (8)$$

This potential restricts the dynamics to two dimensions and we may take the wavefunction of the BEC in the third direction to be constant and Gaussian. Then the energy can be written as :

$$E_{2D} = \int d^2\mathbf{r} \sum_{\sigma=1,2} [-\frac{\hbar^2}{2m}\nabla^2\psi_\sigma(\mathbf{r}) + V_\sigma(\mathbf{r})|\psi_i(\mathbf{r})|^2 + \frac{U_{2D}}{2}|\psi_\sigma(\mathbf{r})|^4] + W_{2D}|\psi_1(\mathbf{r})|^2|\psi_2(\mathbf{r})|^2 \quad (9)$$

where $U_{2D} = U_{3D}\sqrt{\frac{\sqrt{m_{Rb}V_{1D}}\ 2\pi}{\lambda_{1D}\ h}}$ and $W_{2D} = W_{3D}\sqrt{\frac{\sqrt{m_{Rb}V_{1D}}\ 2\pi}{\lambda_{1D}\ h}}$. In the experiment [1], $\lambda_{1D} = \lambda_L =$ 830 nm and $V_{1D} = 8.8E_R$. For these parameters, the weakest lattice yielding a Mott state is $V_{\rm lat} \approx 3.5\mathrm{E_R}$ for two particles per unit cell within the Gutzwiller mean field approximation [5].

From the time-of-flight images obtained, the experimentalists observe a breakdown of the six-fold rotational symmetry in momentum space for lattice depths, $V_{\rm lat}$ ranging from about 1 to 4 E_R, where $E_R = \frac{\hbar^2}{2m_{Rb}\lambda_L^2}$ (m_{Rb} is the mass of ^{87}Rb atoms).

We assume a form of $\psi_1(\mathbf{r})$ and $\psi_2(\mathbf{r})$ which is consistent with the time-of-flight measurements :

$$\psi_1(\mathbf{r}) = \sum_k \psi_1(\mathbf{k})\exp(-i\ \mathbf{k}.\mathbf{r}), \quad (10)$$

$$\psi_2(\mathbf{r}) = \sum_k \psi_2(\mathbf{k})\exp(-i\ \mathbf{k}.\mathbf{r}). \quad (11)$$

where $\mathbf{k}$ are the reciprocal lattice vectors of a honeycomb lattice. We insert this variational ansatz into eq.(4) and minimize the energy with respect to the set of variational parameters $\psi_1(\mathbf{k})$ and $\psi_2(\mathbf{k})$. We find from our simulations that for all experimental parameters $\psi_1(k) = \psi_2^*(\mathbf{k})$, where $\psi_2^*(\mathbf{k})$ is the complex conjugate of $\psi_2(\mathbf{k})$. This result is sensible and implies ψ_1 and ψ_2 are related by a lattice translation.

We perform the variational minimization in Fourier space rather than real space (where such minimization is usually done). This is equivalent to solving the Gross-Pitaevskii equation in real space within a single unit cell with periodic boundary conditions. Computationally, we find momentum space to be more efficient. Moreover, the experimental probes are all in momentum space.

III. METHOD

In k-space, the energy expression, eq.(9) becomes :

$$\frac{E_{2D}}{E_R} = \sum_{\{\mathbf{k},\mathbf{k_1},\mathbf{k_2},\mathbf{k_3}\}\epsilon\overline{\mathcal{L}}} \sum_{i=1,2} [3\ k^2\psi_i^*(\mathbf{k})\psi_i(\mathbf{k}) + V_i(\mathbf{k_1})\psi_i^*(\mathbf{k_2})\psi_i(\mathbf{k_2}-\mathbf{k_1}) + \frac{U}{2}\psi_i^*(\mathbf{k_1})\psi_i^*(\mathbf{k_2})\psi_i(\mathbf{k_3})\psi_i(\mathbf{k_1}+\mathbf{k_2}-\mathbf{k_3})] + W\psi_1^*(\mathbf{k_1})\psi_1(\mathbf{k_2})\psi_2^*(\mathbf{k_3})\psi_2(\mathbf{k_1}+\mathbf{k_3}-\mathbf{k_2}), \quad (12)$$

where $\overline{\mathcal{L}}$ stands for the reciprocal lattice i.e $\mathbf{k} = (\mathrm{a_1}\mathbf{b_1} + \mathrm{a_2}\mathbf{b_2})$, where $\mathrm{a_1}$ and $\mathrm{a_2}$ are integers. One can also generate this lattice from one of $\mathbf{b1}$, $\mathbf{b2}$ and $\mathbf{b3}$, all explicitly given following Eq.(7). All energies (V_i, U and W) are adimensionalized by E_R.

While we carried out unrestricted minimizations, our results are best illustrated by considering an ansatz where the low momentum physics is characterized by 2 complex numbers t and z. In particular, we take $\psi_1(\mathbf{k}) = \mathrm{t}$ and $\psi_2(\mathbf{k}) = \mathrm{z}$ for $\mathbf{k} = \{\mathbf{b1},\ \mathbf{b2},\ \mathbf{b3}\}$ and $\psi_1(\mathbf{k}) = \mathrm{z}$ and $\psi_2(\mathbf{k}) = \mathrm{t}$ for $\mathbf{k} = \{-\mathbf{b1},\ -\mathbf{b2},\ -\mathbf{b3}\}$. In terms of their real and imaginary parts, we write

$$\mathrm{t} = \mathrm{t_r} + i\ \mathrm{t_i}\ \text{and} \quad (13)$$

$$\mathrm{z} = \mathrm{z_r} + i\ \mathrm{z_i}. \quad (14)$$

The order parameter (OP) for the TSF phase is given by:

$$\mathrm{OP} = \frac{|\mathrm{z}|^2 - |\mathrm{t}|^2}{|\mathrm{z}|^2 + |\mathrm{t}|^2} \quad (15)$$

By construction, OP has a non-zero value in the TSF phase and is zero for a uniform condensate. Soltan-Panahi *et al.* measure this order parameter in their experiment to demonstrate the presence of the TSF phase.

For our minimization, we restrict ourselves to $|\mathbf{k}| \leq 6$ giving us 159 complex variational parameters. We find that there are no differences if we use $|\mathbf{k}| \leq 4$ instead (62 variational parameters). Therefore, we believe our results faithfully reflect what would be found if an infinite number of Brillouin zones were included. We gain further confidence in the convergence of our results by noting that the fraction of population occupying the $|\mathbf{k}| = 5$ state when $U = 0.05E_R$ and $V_{\rm lat} = 3.8E_R$ is about 0.1%. In our simulations, we vary U in the range $0.04E_R$ to $U = 0.2E_R$ corresponding to various strengths of the transverse confinement. We also vary α in the range 0.08 to 0.3, corresponding to varying amounts of detuning of the laser beams.

IV. RESULTS

We do not find any evidence for the existence of the Twisted Superfluid phase despite an extensive search of the parameter space. Since Eq.(12) is a quartic form, it will in general have multiple minima and a number of other stationary points. The most grave concern with our results is that we might not have found the global minimum. To some extent, we can alleviate this concern by noting that the experiment finds a continuous symmetry breaking as a function of lattice depth. It therefore suffices to establish that our solution is a dynamically stable local minimum which is continuously connected to the symmetry-unbroken ground state at $V_{\rm lat} = 0$.

A. Local Energetic Stability

We check whether whether we have found a true minimum by looking at the eigenvalues of the Hessian. The Hessian H is a matrix whose elements are given by :

$$H_{ij} = \frac{\partial^2 E}{\partial a_i \partial a_j}, \tag{16}$$

where a_i and a_j are real variational parameters (corresponding to the real and imaginary parts of $\psi(\mathbf{k})$). We find that for all parameters, the eigenvalues of H are positive. This implies that we have at least found a local minimum. In Figure 3, we plot the minimum eigenvalues of the Hessian for different values of the lattice depth ($V_{\rm lat}$) at the illustrative interaction strength, $U = 0.05E_R$ and $\alpha = 0.14$, for five particles (of each species) per unit cell.

We further illustrate the stability of our theory by doing two separate numerical experiments :

(a) Fix the ratio of z_r (Re[z]) to t_r (Re[t]) and vary the remaining variational parameters to find the energy minima. We find that the minimum of the energy occurs when $z_r : t_r = 1$ and there are no other local minima. The dotted curve shows this in Figure 4.

(b) Fix the ratio of z_i (Im[z]) to t_i (Im[t]) and vary the remaining variational parameters to find the energy minima. We find that the minimum of the energy occurs when $z_i : t_i$ =1 and there are no other local minima. The solid curve shows this in Figure 4.

We conclude that there is no second order phase transition within mean field theory.

B. Local Dynamic Stability

We also check whether the minima found is unstable against perturbations. This is done by looking at the

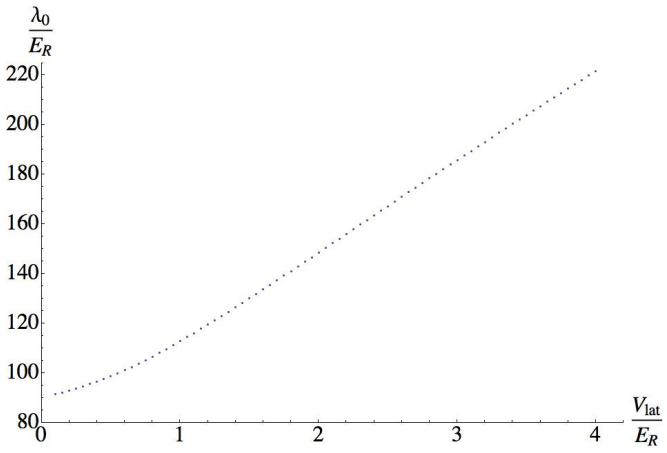

FIG. 3. Minimum eigenvalue of the Hessian, λ_0 in the Normal superfluid phase plotted against the lattice depth, $V_{\rm lat}$ (in units of E_R) when $U = 0.05E_R$ and 5 particles (of each species) are present per unit cell. All the eigenvalues of the Hessian are positive, thereby showing the stability of the normal phase. We conclude that there is no Twisted superfluid phase for these potential depths. This result is illustrative of all parameter ranges we explored.

Gross-Pitaevskii equation :

$$i\hbar \frac{\partial \psi}{\partial t} = \frac{\partial E}{\partial \psi^*} \tag{17}$$

This would imply :

$$i\hbar \frac{\partial \delta a_j}{\partial t} = \frac{\delta E}{\delta a_j} \approx \sum_l \frac{\partial^2 E}{\partial a_j \partial a_l} \delta a_l \tag{18}$$

Taking the real and imaginary parts of both sides, we get the eigenvalue equations

$$\hbar\omega \;\; u = Mu \tag{19}$$

where,

$$M = \begin{bmatrix} \text{Re}[H] & \text{-Im}[H] \\ \text{Im}[H] & \text{Re}[H] \end{bmatrix}$$

We look at the eigenvalues of this matrix, M. A complex eigenvalue would signify the presence of a mode which will grow with time, thus rendering this ground state unstable. We find that all the eigenvalues are real. Thus, the minimum that we have found is also dynamically stable. This is a generic feature of quantum systems: Energetic stability implies dynamic stability [6].

V. BEYOND MEAN FIELD THEORY

In order to explain the experimental observations, one clearly must go beyond our model. One possible direction is including fluctuation effects. These become large

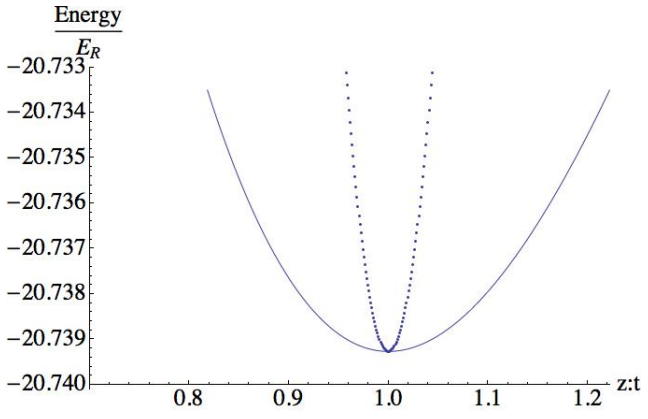

FIG. 4. Slice through the energy landscape at $V_{\rm lat} = 1.8E_R$ and $U = 0.05E_R$ and 5 particles (of each species) per unit cell. Dotted curve: The ratio Re[z]:Re[t]is varied and the energy is found by minimizing with respect to the other variational parameters. Solid curve: Same, but with varying Im[z]:Im[t]. We find that the overall energy minimum occurs when Re[z] = Re[t] and Im[z] = Im[t].

as one approaches the Mott transition (which as previously explained may occur at lattice depths as low as $V_{\rm lat} \approx 3.5E_R$ for two particles per unit cell). In this section, we explore the structure of a more general treatment and evaluate how a twisted superfluid (TSF) could emerge. The most direct approach is is to reduce Eq.(9) to a tight-binding model by writing

$$\psi_\sigma(\mathbf{r}) = \sum_{\rm i} \hat{\rm a}_{\sigma \rm i}\phi(\mathbf{r} - \mathbf{r_i}), \tag{20}$$

where $\hat{a}_{\sigma i}$ annihilates a boson of species σ on site i, at position $\rm r_i$, where $\phi(\mathbf{r} - \mathbf{r_i})$ is the Wannier state wavefunction. With this substitution, the Hamiltonian becomes :

$$H_{\rm full} = H_0 + H_1 + H_2 + \ldots, \tag{21}$$

where H_0 involves only the onsite terms, H_1 involves the nearest neighbors, H_2 involves the next nearest neighbors and so on. Our mean field theory includes all of the terms in Eq.(21). At large lattice depths, the Wannier states are well localized, and each subsequent term in Eq.(21) is smaller. In addition to a large number of other expressions, H_1 contains single particle hopping and pair hopping terms. Neglecting the spin index, these terms are

$$H^{(\rm sph)} = -{\rm t}(\hat{\rm a}_{\rm i}^\dagger \hat{\rm a}_{\rm j} + \hat{\rm a}_{\rm j}^\dagger \hat{\rm a}_{\rm i}) \tag{22}$$

and

$$H^{(\rm ph)} = {\rm t}'(\hat{\rm a}_{\rm i}^\dagger \hat{\rm a}_{\rm i}^\dagger \hat{\rm a}_{\rm j}\hat{\rm a}_{\rm j} + \hat{\rm a}_{\rm j}^\dagger \hat{\rm a}_{\rm j}^\dagger \hat{\rm a}_{\rm i}\hat{\rm a}_{\rm i}) \tag{23}$$

respectively. Within mean field theory, these terms give a contribution to the energy

$$H^{(\rm sph)} + H^{(\rm ph)} = 3\left(-{\rm t}\sqrt{{\rm n}_+{\rm n}_-}{\rm Cos}(\delta) + {\rm t}'{\rm n}_+{\rm n}_-{\rm Cos}(2\delta)\right), \tag{24}$$

where $\langle \hat{\rm a}_{\rm j\pm}\rangle = \sqrt{{\rm n}_\pm}\exp(\pm {\rm i}\ \delta/2)$, where the + and - signs are taken on the distinct triangular sub-lattices. This approximation neglects much of the physics included in sections III and IV, but nicely explains a mechanism for developing a TSF. Namely, if $(4{\rm t}'{\rm n}_+{\rm n}_- > {\rm t}\sqrt{{\rm n}_+{\rm n}_-})$, Eq.(24) is minimized by making $\delta \neq 0$ (cf. Methods section of [1]). As illustrated by the absence of a TSF in the full mean field theory, the neglected terms must suppress this symmetry breaking. One could however imagine that Mott physics may renormalize parameters and change this result. For example, Mott physics will send $H^{(\rm sph)}$ to zero in the insulating phase, while having a smaller effect on terms such as counterflow hopping:

$$H^{(\rm cf)} = {\rm t}_{\rm cf}\sum_{<{\rm ij}>}(\hat{\rm a}_{\rm i\uparrow}^\dagger \hat{\rm a}_{\rm j\downarrow}^\dagger \hat{\rm a}_{\rm j\uparrow}\hat{\rm a}_{\rm i\downarrow} + \hat{\rm a}_{\rm i\downarrow}^\dagger \hat{\rm a}_{\rm j\uparrow}^\dagger \hat{\rm a}_{\rm j\downarrow}\hat{\rm a}_{\rm i\uparrow}) \tag{25}$$

If such terms are responsible for the TSF, then the experimental observations can be interpreted as a signature of "transverse" magnetic ordering or at least short range magnetic correlations.

One could experimentally explore the importance of quantum fluctuations by changing the strength of the transverse confinement, $V_{\rm conf}(\mathbf{r})$. This impacts the onsite interaction while leaving the hopping largely unaffected. Systematically studying the order parameter as a function of lattice depth and transverse confinement may provide the key to understand this phenomenon.

Another direction worth exploring is the modeling of the time-of-flight expansion or the turn-off of the optical lattice. Phases accumulated during the expansion could mimic a TSF. Estimates of these phases suggest however that they are too small [7].

ACKNOWLEDGEMENTS

This paper is based on work supported by the National Science Foundation under Grant no. PHY-1068165.

[1] P. Soltan-Panahi *et al.*, Nature Physics **8**, 71-75 (2012).
[2] J. Struck *et al.*, Science **333**, 996 (2011).
[3] G. Wirth, M. Ölschläger and A. Hemmerich, Nature Physics **7** ,147-153 (2011).

[4] M. Ölschläger, G. Wirth and A. Hemmerich Phys. Rev. Lett. **106**, 015302 (2011).
[5] P. Soltan-Panahi *et al.*, Nature Physics **7**, 434-440 (2011).
[6] C. J. Pethick and H. Smith, *Bose-Einstein Condensation in Dilute Gases*. Cambridge University Press, Cambridge (2002).
[7] J. N. Kupferschmidt and E. J. Mueller , Phys. Rev. A **82**, 023618 (2010).